Biochimica et Biophysica Acta 850 (1986) 436–448
Elsevier

BBA 42039

Rhodamine 123 as a probe of transmembrane potential in isolated rat-liver mitochondria: spectral and metabolic properties

Ronald K. Emaus, Ron Grunwald and John J. Lemasters *

Laboratories for Cell Biology, School of Medicine, University of North Carolina at Chapel Hill, 108 Swing Building 217 H, Chapel Hill, NC 27514 (U.S.A.)

(Received February 25th, 1986)

Key words: Respiration; Electron transport; Fluorescence quenching; Rhodamine 123; Membrane potential; (Rat-liver mitochondria)

The spectral and metabolic properties of Rhodamine 123, a fluorescent cationic dye used to label mitochondria in living cells, were investigated in suspensions of isolated rat-liver mitochondria. A red shift of Rhodamine 123 absorbance and fluorescence occurred following mitochondrial energization. Fluorescence quenching of as much as 75% also occurred. The red shift and quenching varied linearly with the potassium diffusion potential, but did not respond to ΔpH. These energy-linked changes were accompanied by dye uptake into the matrix space. Concentration ratios, in-to-out, approached 4000:1. A large fraction of internalized dye was bound. At concentrations higher than those needed to record these spectral changes, Rhodamine 123 inhibited ADP-stimulated (State 3) respiration of mitochondria (K_i = 12 μM) and ATPase activity of inverted inner membrane vesicles (K_i = 126 μM) and partially purified F_1-ATPase (K_i = 177 μM). The smaller K_i for coupled mitochondria was accounted for by energy-dependent Rhodamine 123 uptake into the matrix. Above about 20 nmol/mg protein (10 μM), Rhodamine 123 caused rapid swelling of energized mitochondria. Effects on electron-transfer reactions and coupling were small or negligible even at the highest Rhodamine 123 concentrations employed. Δψ-dependent Rhodamine 123 uptake together with Rhodamine 123 binding account for the intense fluorescent staining of mitochondria in living cells. Inhibition of mitochondria ATPase likely accounts for the cytotoxicity of Rhodamine 123. At concentrations which do not inhibit mitochondrial function, Rhodamine 123 is a sensitive and specific probe of Δψ in isolated mitochondria.

Introduction

The laser dye, Rhodamine 123, has been extensively employed as a fluorescent stain of mitochondria in living cells [1–6]. Since Rhodamine 123 is an aromatic cation, it has been assumed, although never directly demonstrated, that Rhodamine 123 distributes electrophoretically into the mitochondrial matrix in response to Δψ. Agents known to depolarize or deenergize mitochondria, such as uncouplers and respiratory inhibitors, decrease Rhodamine 123 fluorescence of mitochondria in cultured cells, whereas agents which collapse ΔpH and hyperpolarize Δψ, such as nigericin, increase fluorescence [2,3]. In isolated mitochondria, there is no work relating Δψ to the uptake and spectral properties of Rhodamine 123.

Rhodamine 123 is described as less toxic to

* To whom correspondence should be addressed.

Abbreviations: CCCP, carbonyl cyanide *m*-chlorophenylhydrazone, DASPMI, dimethylaminostyrylmethylpyridinium iodide, Hepes, 4-(2-hydroxyethyl)-1-piperazineethanesulfonic acid; P_i, inorganic phosphate; CMC, critical micellar concentration.

0005-2728/86/$0.350 © 1986 Elsevier Science Publishers B.V. (Biomedical Division)

cells than other fluorescent cations which have been used to stain mitochondria [1,2]. At high concentrations, however, Rhodamine 123 is cytotoxic. Rhodamine 123 has also been reported to be selectively more toxic to transformed and carcinoma cell lines than to normal cells, a phenomenon correlated with increased accumulation and retention of Rhodamine by transformed and carcinoma cells [4,6–9]. In isolated mitochondria, Rhodamine 123 inhibits mitochondrial metabolism, particularly the mitochondrial ATPase [10–12]. However, differences in susceptibility to Rhodamine 123 by isolated mitochondria from Rhodamine 123-sensitive and resistant cells did not account for differential toxicity [13].

In this communication, we describe the mechanism of Rhodamine 123 uptake into isolated rat-liver mitochondria in relation to the spectral properties of Rhodamine 123 after uptake and the effects of Rhodamine 123 on mitochondrial metabolism. We show that Rhodamine 123 is taken up in response to $\Delta\psi$, although with substantial binding to internal mitochondrial components, and that Rhodamine 123 uptake is accompanied by red spectral shifts and quenching of fluorescence. The metabolic effects of Rhodamine 123 are magnified by uptake and include an inhibition of mitochondrial ATPase and a disruption of mitochondrial volume control, the latter possibly by an independent mechanism. A brief description of this work has appeared earlier [11].

Materials and Methods

Mitochondrial isolations. Rat liver mitochondria were isolated in 0.25 M sucrose, 2 mM potassium-Hepes buffer (pH 7.4) [14]. In some experiments 2 mM sodium Hepes buffer was used instead. Inverted inner membrane vesicles were prepared by sonication of digitonin mitoplasts [15]. Partially purified F_1-ATPase was prepared by chloroform extraction of inverted inner membrane vesicles [16]. Protein was determined by a biuret procedure [17] for mitochondria and vesicles and by the Lowry method [18] for F_1-ATPase employing crystalline bovine serum albumin as standard.

Absorbance and fluorescence measurements. Absorbance measurements were made with an Aminco DW-2a dual-wavelength spectrophotometer or, at high concentrations of Rhodamine 123, with a Hewlett-Packard 8150A Diode Array Spectrophotometer using 0.1 or 0.2 mm cuvettes. Fluorescence, 90° light-scattering, and polarization measurements were made with a Perkin-Elmer 650-40 Fluorescence Spectrophotometer. Polarization was defined as $(I_{\parallel} + I_{\perp})/(I_{\parallel} + I_{\perp})$. During spectral measurements, reaction media containing mitochondria were stirred continuously with a magnetic flea.

Enzyme assays. Oxygen uptake during respiration was measured with a Clark electrode in a glass reaction vessel. Respiratory control in inverted inner membrane vesicles oxidizing NADH was determined as the ratio of the rate of respiration in the presence of CCCP plus oligomycin to that in the presence of oligomycin alone [19]. ATPase activity was determined by coupled enzyme assay as described previously [19]. All incubations were carried out at 23°C.

Calculation of $\Delta\psi$. Membrane potentials (negative inside) were calculated by the Nernst equation:

$$\Delta\psi = 59 \log \frac{[X]_{in}}{[X]_{out}} \quad (1)$$

where $[X]$ is either Rhodamine 123 or K^+. $[K^+]_{in}$ was assumed to be 120 mM [20]. [Rhodamine 123]$_{in}$ was estimated from Rhodamine 123 uptake assuming distribution into a matrix space of 1 μl/mg of protein [21].

Chemicals. Rhodamine 123 (laser grade) was obtained from Eastman Kodak Co. and used without further purification. Other reagents and chemicals were obtained from standard commercial sources.

Results

Red shift of Rhodamine 123 absorbance and fluorescence spectra due to energization of the mitochondrial membrane

Rat liver mitochondria were incubated with succinate and 2.6 μM Rhodamine 123 under State 4 conditions. After an absorbance spectrum was recorded, the mitochondria were uncoupled with 2 μM CCCP. Compared to the uncoupled suspension, coupled mitochondria were red-shifted 11

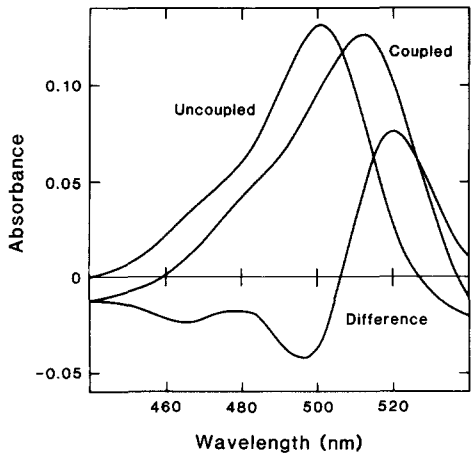

Fig. 1. Red shift of Rhodamine 123 absorbance due to mitochondrial energization. Rat liver mitochondria (0.4 mg/ml of protein) were added to succinate-containing medium and a baseline recorded. Absorbance spectra were collected after the sequential addition of 2.62 μM Rhodamine 123 (Coupled) and 2 μM CCCP (Uncoupled). The difference spectrum (Difference), coupled minus uncoupled, was calculated manually. Other components to the reaction medium were 150 mM sucrose/5 mM $MgCl_2$/5 mM disodium succinate/2.5 μM rotenone/5 mM KP_i buffer/20 mM potassium-Hepes buffer (pH 7.4).

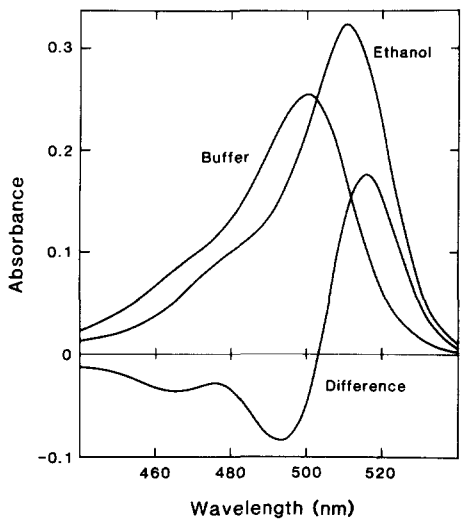

Fig. 2. Red shift of Rhodamine 123 absorbance in ethanolic solution. Absorbance spectra were collected for 3.81 μM Rhodamine 123 in aqueous 20 mM potassium-Hepes buffer (pH 7.4) (Buffer), in absolute ethanol (Ethanol), and for the absorbance difference of ethanol-minus-aqueous buffer (Difference).

nm (Fig. 1). The coupled-minus-uncoupled difference spectrum had a maximum at 516 and a minimum at 495 nm. The uncoupled spectrum was virtually identical to the aqueous absorbance spectrum of Rhodamine 123, whereas the coupled spectrum resembled the ethanolic spectrum (Fig. 2). The red shift in absorbance was easily recognized by visible changes in the color of mitochondrial suspensions which changed from orange during energization (coupled) to yellow after deenergization (uncoupled).

Changes in pH between 2 and 10 did not significantly alter the absorbance maximum of Rhodamine 123 and thus could not account for the large shift observed in coupled mitochondria. There was also no evidence of dye stacking in aqueous solution, since the absorbance maximum and extinction coefficient remained unchanged to concentrations of 3.5 mM, near the solubility limit of Rhodamine 123.

Rhodamine 123 in aqueous solution had a fluorescence excitation maximum at 500 nm and an emission maximum at 525 nm (Fig. 3, Table I). In

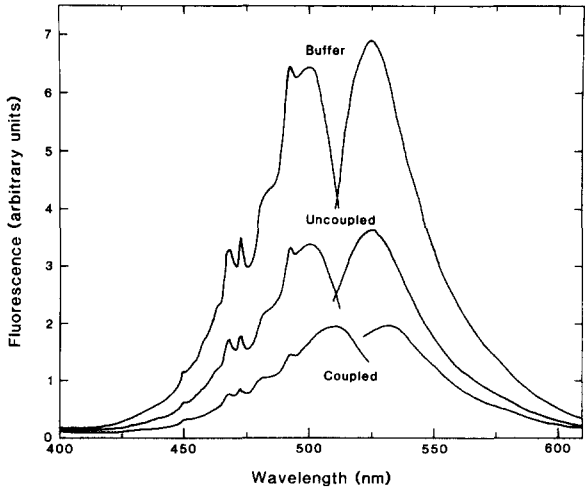

Fig. 3. Red shift and quenching of Rhodamine 123 fluorescence following mitochondrial energization. Uncorrected Rhodamine 123 excitation and emission spectra were obtained in reaction medium without mitochondria (Buffer), with mitochondria (Coupled) and with mitochondria plus 2 μM CCCP (Uncoupled). The excitation peaks at 467, 473, 483 and 492 nm were due to the lamp source, Concentrations of Rhodamine 123 and mitochondria were 0.47 μM and 0.17 mg/ml of protein, respectively. Other components of the reaction medium were as described in Fig. 1.

TABLE I

UNCORRECTED EXCITATION AND EMISSION MAXIMA FOR RHODAMINE 123 FLUORESCENCE UNDER VARIOUS CONDITIONS

Reaction media contained 0.285 μM Rhodamine 123 and 10 mM potassium-Hepes (pH 7.4) except at noted. Relative fluorescence intensity is expressed with reference to aqueous buffer at equal Rhodamine 123 concentration. CTMA, cetyltrimethylammonium.

Condition	Excitation maximum (nm)	Emission maximum (nm)	Relative fluorescence intensity (%)
Buffer [a]	500	525	100
Coupled mitochondria [a]	511	532	28.5
Uncoupled mitochondria [a]	501	525	52.6
Absolute ethanol	511	530	136
20 mM SDS (CMC, 8.2 mM)	510	531	86.2
2 mM SDS	499	524	48.3
0.8 mM Triton X-100 (CMC, 0.24 mM)	499	524	99.5
0.08 mM Triton X-100	499	524	105
2.5 mM CTMA (CMC, 0.92 mM)	499	525	98.7
0.2 mM CTMA	499	525	105
20 mM ATP	502	528	41.4

[a] Conditions are described in Fig. 3.

the presence of energized mitochondria, both excitation and emission maxima shifted to the red. In contrast to mitochondria in living cells which are made intensely fluorescent by Rhodamine 123, fluorescence of isolated mitochondrial suspensions was quenched by energization. Percent quenching

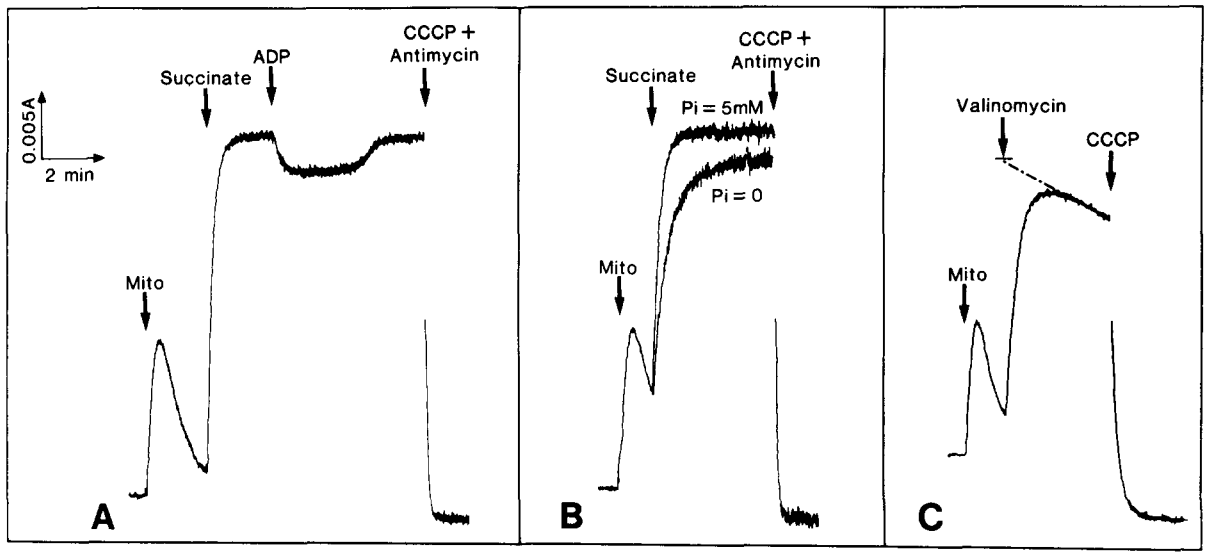

Fig. 4. Mitochondrial energization monitored by the absorbance red shift of Rhodamine 123. Absorbance was measured by dual-wavelength spectrophotometry at 516 minus 495 nm in basic reaction medium containing 150 mM sucrose/5 mM $MgCl_2$/3.2 μM rotenone/0.6 μM Rhodamine 123/5 mM KP_i buffer/20 mM potassium-Hepes buffer (pH 7.4). In (A) additions were 0.4 mg protein per ml rat-liver mitochondria/5 mM disodium succinate/200 μM ADP/1.6 μM CCCP/1.6 μg/ml antimycin. In (B) the basic reaction medium contained 0 or 5 mM KP_i as indicated. Other additions were as described in (A). In (C) sodium Hepes and NaP_i buffers replaced potassium-Hepes and KP_i. Mannitol, 39.8 mM, and 0.13 mM KCl were also present. Additions were 20 ng/ml valinomycin and as described in (A).

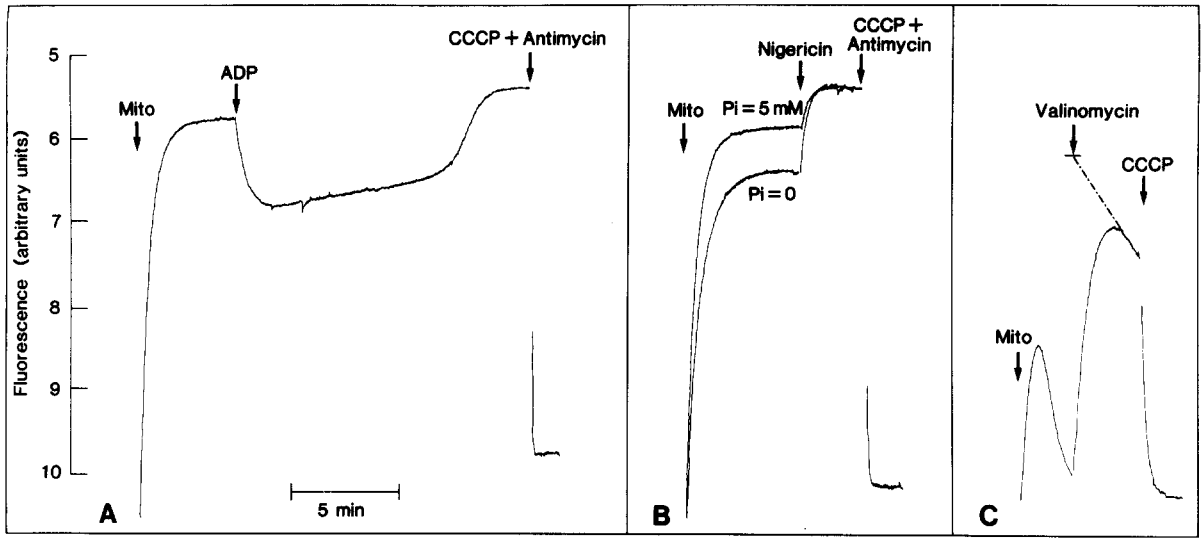

Fig. 5. Mitochondrial energization monitored by fluorescence quenching of Rhodamine 123. Fluorescence excited at 503 nm (2 nm slit) and emitted at 527 nm (3 nm slit) was measured in basic reaction medium containing 150 mM sucrose/5 mM $MgCl_2$/5 mM disodium succinate/2.7 μM rotenone/0.2 μM Rhodamine 123/5 mM KP_i buffer/20 mM potassium-Hepes buffer (pH 7.4). In (A), additions were 0.167 mg protein per ml rat-liver mitochondria/300 μM ADP/1.3 μM CCCP/1.3 μg per ml antimycin. In (B) the basic reaction medium contained 0 or 5 mM KP_i as indicated. Additions were 67 ng/ml nigericin and as described in (A). In (C) sodium-Hepes and NaP_i buffers replaced potassium-Hepes and KP_i. 39.8 mM mannitol and 0.1 mM KCl were also present, and succinate was absent. Additions were 20 ng/ml valinomycin and as described in (A).

was virtually independent of Rhodamine 123 concentration. Whereas quenching was only partially reversed by uncoupler, the red shifts of the excitation and emission spectra were fully reversed. In ethanol, fluorescence was also red-shifted, but its intensity increased rather than decreased to 136% of its aqueous value (Table I).

The energetic status of mitochondria could be monitored both by absorbance measured at the wavelength pair 516 minus 495 nm (Fig. 4) and by fluorescence quenching (Fig. 5). In the absence of oxidizable substrate, absorbance and fluorescence changes indicated a transient, incomplete energization following addition of mitochondria to the reaction medium. This effect was presumably due to oxidation of endogenous substrate (Fig. 4A–C, Fig. 5C). After addition of succinate, a respiratory substrate, full and sustained energization was indicated by the dye responses (State 4). After ADP, $\Delta A_{516-495}$ and fluorescence quenching decreased as ATP synthesis occurred (State 3). Upon complete conversion of added to ADP to ATP, absorbance and fluorescence returned close to their previous State-4 levels. Deenergization with uncoupler (CCCP) and respiratory inhibitor (antimycin) produced rapid reversal of the energy-linked absorbance red shift and fluorescence quenching (Figs. 4A and 5A).

The data suggested that Rhodamine 123 was responding to $\Delta\tilde{\mu}_{H^+}$ or one of its components, $\Delta\psi$ or ΔpH. As a permeant weak acid, P_i tends to collapse ΔpH and cause a compensatory increase in $\Delta\psi$. Since the absorbance red shift and fluorescence quenching were greater in the presence of 5 mM P_i than in its absence (Fig. 4B and 5B), Rhodamine 123 appeared to be responding to the $\Delta\psi$ component of $\Delta\tilde{\mu}_{H^+}$. Nigericin, which also collapses ΔpH and hyperpolarizes $\Delta\psi$, also produced an increase in fluorescence quenching (Fig. 5B). However, absorbance behaved anomalously after nigericin addition. There was a rapid small decrease as well as a decrease in the baseline after deenergization (data not shown). These data suggested some type of direct interaction of nigericin with Rhodamine 123 producing a small absorbance shift, but the phenomenon was not investigated further.

$\Delta\psi$ and spectral changes of Rhodamine 123

Absorbance and red shifts and fluorescence quenching also occurred in response to valinomycin-induced potassium diffusion potentials (Figs, 4C and 5C). After initial increases, absorbance red shifts and fluorescence quenching decreased linearly owing to depletion of mitochondrial potassium and consequent decay of $\Delta\psi$. The higher the initial $\Delta\psi$, the more rapid was the decay. Formation of $\Delta\psi$ after addition of valinomycin is expected to be virtually instantaneous, and the 1–2 min required for maximum absorbance and fluorescence changes to occur was a reflection of the response time of the dye to $\Delta\psi$.

Absorbance red shifts and fluorescence quenching were calibrated to the valinomycin-induced potassium diffusion potential by extrapolating backwards to the time of valinomycin addition as illustrated in Figs. 4C and 5C. The absorbance red shift and the degree of fluorescence quenching both varied linearly with $\Delta\psi$ (Fig. 6). Values for $\Delta\psi$ (negative inside) were calculated assuming an internal K^+ concentration of 120 mM [20]. The calibration curves intersected the $\Delta\psi$ axis above zero indicative of a residual potential for nonenergized mitochondria. In different experiments, the fluorescence data indicated residual potentials between 55 and 65 mV, whereas the absorbance data indicated residual potentials between 15 and 50 mV. Plots of the maximum changes of absorbance and fluorescence without extrapolation were also linear with the potassium diffusion potential and indicated similar residual potentials (data not shown).

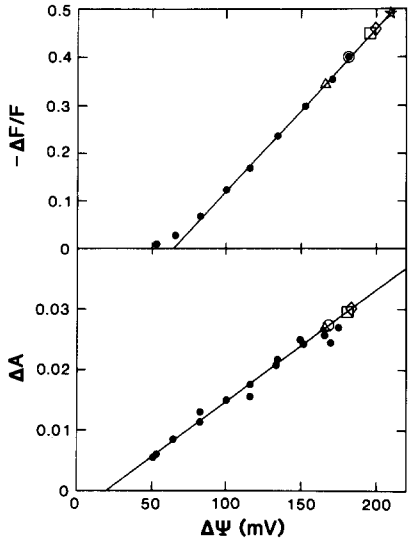

Fig. 6. Rhodamine 123 spectral changes and potassium diffusion potentials in rat-liver mitochondria. Rhodamine 123 absorbance and fluorescence signals were extrapolated backwards to the time of valinomycin addition as illustrated in Figs. 4C and 5C. ΔA and ΔF are differences between extrapolated absorbance and fluorescence values and values obtained after CCCP. F is fluorescence after CCCP. $\Delta\psi$ was varied by varying KCl between 0.1 and 16 mM and mannitol between 39.8 mM and 8 mM. Open symbols show where mitochondria incubated under various metabolic conditions fall on the calibration curve: □, plus succinate (State 4); △, plus succinate and ADP (State 3); ○, plus succinate without added P_i; *, plus succinate and nigericin; ◇, plus 5 mM glutamate and 5 mM malate (State 4). Conditions were as described in Figs. 4 and 5.

From Fig. 6, $\Delta\psi$ for succinate-supported State-4 respiration was 181 mV from the absorbance red shift and 197 mV from fluorescence quenching. For glutamate plus malate-supported respiration, the respective values were 183 mV and 199 mV. After ADP, absorbance indicated a 15 mV drop in $\Delta\psi$, whereas fluorescence indicated a 22 mV decrease.

Factors affecting the spectral properties of Rhodamine 123

The disparity of $\Delta\psi$ estimated from absorbance red shifts and from fluorescence quenching suggested that other factors may contribute to the spectral responses of Rhodamine 123. Quenching in the absence of mitochondria occurred in the presence of ADP and ATP with nearly maximal quenching occurring at nucleotide concentrations above 20 mM. Downward-curving Stern-Volmer plots were consistent with a static quenching mechanism rather than classical bimolecular collisional quenching (Fig. 7). Magnesium ion in molar excess over nucleotide reduced, but did not eliminate quenching.

At high ATP and ADP, a 2–3 nm red shift in fluorescence excitation and emission maxima was observed (Table I). There was a similar red shift in the absorbance spectrum which produced a difference spectrum qualitatively similar to that observed in coupled-vs.-uncoupled mitochondria. The magnitude of the red-absorbance shift induced by adenine nucleotide, however, was much

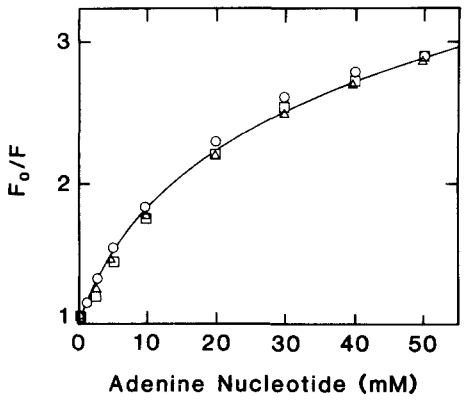

Fig. 7. Stern-Volmer plot of adenine nucleotide quenching of Rhodamine 123 fluorescence. Fluorescence excited at 500 nm and emitted at 525 nm was measured in aqueous medium containing 0.285 μM Rhodamine 123, 10 mM potassium-Hepes buffer (pH 7.4) and 0–50 mM ATP (circles), ADP (triangles) or ATP plus 5mM $MgCl_2$ (squares). F_0/F is the ratio of fluorescence in the absence of nucleotide to that in its presence.

smaller than that caused by mitochondrial energization.

Rhodamine 123 fluorescence was also altered by the anionic detergent, SDS (Table I). Below the critical micellar concentrations, Rhodamine 123 fluorescence was strongly quenched. Above the critical micellar concentration, Rhodamine 123 fluorescence regained most of its original value in the absence of detergent, but the excitation and emission maxima were red-shifted to 510 and 531 nm, respectively, values corresponding to those found in energized mitochondria (Table I). Rhodamine 123 fluorescence was not affected by neutral Triton X-100 or cationic cetyl trimethyl ammonium detergents above or below their critical micellar concentrations (Tabel I). Bulk phase experiments in which Rhodamine 123 was partitioned against heptane revealed that aqueous Rhodamine 123 was essentially insoluble in the nonpolar solvent at neutral pH. Thus, Rhodamine 123 is amphipathic rather than lipophilic, and the effect of SDS on its spectral properties appears to be due to the anionic nature of the detergent (see Ref. 21).

Rhodamine 123 spectra were recorded in the presence of inside-out inner membrane vesicles with and without energization by ATP or NADH. Energization had no effect on Rhodamine 123 absorbance and fluorescence spectra. Vesicles in the absence of an energy source themselves caused an approx. 30% decrease in fluorescence, but no wavelength shift. Since there was also no wavelength shift in uncoupled mitochondria, it is unlikely that the red shift of Rhodamine 123 absorbance following energization of intact mitochondria was due solely to an interaction Rhodamine 123 with one or the other membrane surface.

Uptake of Rhodamine 123 by rat liver mitochondria

Right-angle light-scattering measurements indicated that mitochondria oxidizing succinate at State 4 swelled rapidly in the presence of more than 20 nmol Rhodamine 123 (10 μM) (data not shown). Safranin, tetraphenylphosponium and triphenylmethylphosphonium, three other cations useful in measuring membrane potentials, did not cause swelling even at 53.4 nmol/mg of protein. Thus, at high concentrations, Rhodamine 123 but not other cationic probes may affect mitochondrial membrane permeability in a fashion which dis-

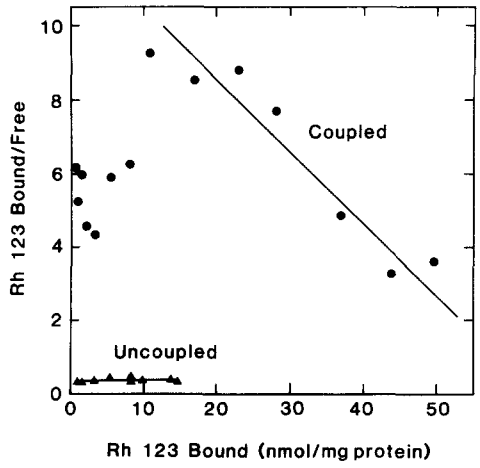

Fig. 8. Scatchard plot of Rhodamine 123 (Rh 123) binding to rat-liver mitochondria. Rat-liver mitochondria, 1 mg of protein/ml, were incubated for 1.5 min with 0.4 to 63 μM Rhodamine 123 in basic reaction medium described in fig. 1. After centrifugation for 5 min at 5000× *g*, free Rhodamine 123 in the supernatant was determined by absorbance at 500 nm. Bound Rhodamine 123 was taken as total minus free. Circles are with no other additions (Coupled). Triangles are with addition of 1 mM KCN, 2 μM CCCP and.2 μg/ml oligomycin (Uncoupled).

rupts normal mitochondrial volume homeostasis.

Direct measurements after centrifugation of Rhodamine 123 bound to coupled and uncoupled mitochondria indicated substantial uptake of dye following energization. State-4 mitochondria bound 75–90% of added Rhodamine 123 in the test range 0.4–63 nmol per mg protein. Uncoupled mitochondria retained 10–30% of the dye. A Scatchard plot of the data was biphasic (Fig. 8). Above 10 nmol Rhodamine 123 bound per mg of protein, the Scatchard plot suggested a single class of binding sites in coupled mitchondria whose concentration was 63 nmol/mg of protein with an apparent binding affinity of $2 \cdot 10^5\ M^{-1}$. Below 10 nmol Rhodamine 123 bound per mg protein, the data points clustered around a bound-to-free ratio of 4–6. The discontinuity of the Scatchard plot occurred near the concentration of Rhodamine 123 which caused rapid swelling. Thus, above this concentration, increased binding was due to an increased matrix volume and hence increased capacity to hold Rhodamine 123 which, in terms of a Scatchard analysis, is equivalent to an increase in the number of binding sites. Linearity of the Scatchard plot, therefore, was not the consequence of uniform high-affinity binding, but was the result of electrophoretic uptake, swelling and subsequent partial uncoupling and decline of $\Delta\psi$ (see Fig. 9). At Rhodamine 123 concentrations which did not cause swelling, bound to free ratios did not change, since at constant volume these ratios are determined by $\Delta\psi$ rather than by the number and affinity of putative binding sites. Filtration experiments also confirmed that the relative amount of dye bound by coupled mitochondria was constant in the 0–2 μM range (Table II). In experiments with uncoupled mitochondria, there was still a significant amount of binding, although the scatter of the data was large, since the absolute amount of Rhodamine 123 bound was smaller. Using the Nernst equation and assuming a matrix volume of 1 μl/mg of protein, $\Delta\psi$ averaged 210 mV for coupled mitochondria and 110 mV for uncoupled.

Rhodamine 123 uptake into energized mitochondria was accompanied by a large increase in fluorescence polarization as compared to uncoupled mitochondria (Table III). A similarly high fluorescence polarization was obtained when Rhodamine 123 was dissolved in 40% fluorescence

TABLE II

BINDING OF RHODAMINE 123 TO COUPLED AND UNCOUPLED RAT LIVER MITOCHONDRIA

In filtration experiments, Rhodamine 123 uptake by rat-liver mitochondria was determined and $\Delta\psi$ calculated according to the Nernst equation assuming a matrix volume of 1 μl/mg protein. Mitochondria, 0.83 mg protein/ml, were filtered through Millipore AAP15 prefilters and 0.2 μm phosphatidyl choline membrane filters after 1.5 min in basic reaction medium described in Fig. 1 Correcting for nonspecific adsorption of Rhodamine 123 to the filters, free Rhodamine 123 in the filtrate was determined from absorbance at 500 nm. Bound Rhodamine 123 was taken as total minus free. Uncoupling was by addition of 1.3 μM CCCP, 2 μg/ml antimycin and 2 μg/ml oligomycin.

Total Rhodamine 123 (μM)	Concentration (μM)		In/Out Ratio	$\Delta\psi$ (mV)
	out	in		
Coupled				
0.1	0.025	90.4	3640	210
0.2	0.053	177	3350	208
0.4	0.102	359	3520	209
0.8	0.202	721	3670	210
1.6	0.374	1480	3950	212
Uncoupled				
0.1	0.080	24.2	303	146
0.2	0.187	15.7	84.0	114
0.4	0.397	3.5	8.9	56
0.8	0.748	62.8	84.0	114
1.6	1.470	160	109	120

TABLE III

FLUORESCENCE POLARIZATION OF RHODAMINE 123

Condition	Polarization
Rhodamine 123 (0.47 μM) in reaction medium [a]	0.016
+ coupled mitochondria (0.17 mg protein/ml)	0.172
+ uncoupled mitochondria [a]	0.027
Rhodamine 123 (0.26 μM) in ethanol [c]	0.038
+ 5% (w/w) glycerol	0.045
+ 10% glycerol	0.047
+ 20% glycerol	0.078
+ 40% glycerol	0.167
+ 50% glycerol	0.223
Rhodamine 123 (0.285 μM) in 10 potassium-Hepes buffer (pH 7.4) [d]	0.018
+ 20 mM SDS	0.076
+ 2 mM SDS	0.021
+ 0.8 mM Triton X-100	0.019
+ 2.5 mM cetyltrimethylammonium	0.028
+ 50 mM ATP	0.057

[a] Excitation and emission wavelengths were 492 and 527 nm, respectively, in reaction medium described in Fig. 1.
[b] Uncoupled with 2 μM CCCP.
[c] Excitation and emission wavelengths were 510 and 530 nm, respectively.
[d] Excitation and emission wavelengths were 500 and 525 nm, respectively.

polarization were observed when Rhodamine 123 was dissolved in water together with high concentrations of adenine nucleotide or with micellar SDS. Triton X-100, cetyltrimethylammonium and monomeric SDS caused negligible changes in polarization. Increased fluorescence polarization suggested a large degree of immobilization or binding of internalized probe. Alternatively, a large decrease in fluorescence lifetime may have been responsible. However after energization, the amount of quenching (46%, see Table I) was not commensurate to the increase in polarization (637%). This favors binding or immobilization of Rhodamine 123 following mitochondrial energization.

Rhodamine 123 and mitochondrial metabolism

Concentrations of Rhodamine 123 below 1 μM had little influence on mitochondrial respiration. Above 1 μM Rhodamine 123 inhibited ADP-stimulated (State 3) respiration with 12 μM causing a half-maximal effect (Fig. 9). At higher concentrations, uncoupled rates declined by a small amount and State-4 rates increased slightly. Both effects may be related to swelling, since NADH oxidation and respiratory control by inverted inner membrane vesicles were not affected at these higher concentrations (Table IV). The data of Fig. 9 were obtained with glutamate plus malate as respiratory substrate, but essentially identical results were obtained with succinate.

TABLE IV

INHIBITION BY RHODAMINE 123 OF VARIOUS MITOCHONDRIAL ENZYME ACTIVITIES

Activity	K_i (μM)
F_1-F_0-ATPase (oligomycin-sensitive) of inverted inner membrane vesicles	126
F_1ATPase (oligomycin-insensitive), partially purified	177
Uncoupled NADH-supported respiration of inverted inner membrane vesicles	≫ 190
Uncoupler/oligomycin respiratory control ratio of inverted inner membrane vesicles	≫ 190

The inhibition of State-3 respiration by Rhodamine suggested an interaction with the

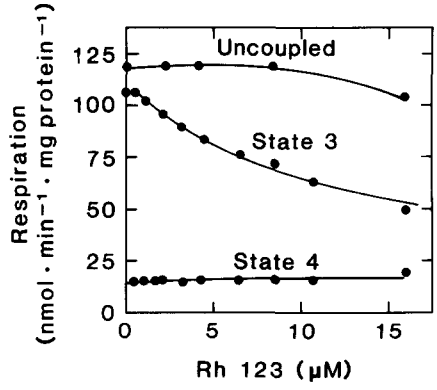

Fig. 9. Inhibition of mitochondrial respiration by Rhodamine 123 (Rh 123). Oxygen uptake by rat-liver mitochondria was measured after no additions (State 4), after 267 μM ADP (State 3) and after 27 μM dinitrophenol (DNP) in reaction medium containing 150 mM sucrose/5 mM $MgCl_2$/5 mM sodium glutamate/5 mM sodium malate/0.83 mg protein per ml rat liver mitochondria/10 mM KP_i buffer/20 mM potassium-Hepes buffer (pH 7.4).

mitochondrial ATPase. An inhibitor titration of F_1F_0-ATPase activity in inverted inner membrane vesicles demonstrated Rhodamine 123 inhibition with an apparent K_i of 126 μM (Table IV). A similar half-maximal inhibition was observed for partially purified oligomycin-insensitive F_1-ATPase (Table IV).

Discussion

Two major changes in the spectral properties of Rhodamine 123 were observed during incubation with isolated rat liver mitochondria. The first was an energy-dependent red shift of the absorbance and fluorescence excitation and emission spectra. The shift was 10–11 nm for absorbance and excitation and somewhat less for emission. A similar shift in the fluorescence excitation spectrum has been described for Rhodamine 123 incubated with whole living cells [5]. Following our initial report [11], Modica-napolitano and co-workers [12] also noted an energy-linked change in absorbance. The second spectral change was an energy-dependent quenching of fluorescence. These spectral changes could be monitored continuously by dual-wavelength spectrophotometry and by fluorescence spectroscopy at fixed emission and excitation wavelengths. Both red shift and quenching varied linearly with valinomycin-induced potassium diffusion potentials. The dye responses appeared insensitive to ΔpH and indicated the expected hyperpolarization when ΔpH was diminished by high P_i. A related compound, rhodamine 6G, has been reported to show similar energy-linked optical changes [23,24]. Unlike Rhodamine 123, rhodamine 6G absorbance decreased following energization in addition to undergoing a red shift.

The energy-linked absorbance and fluorescence changes were accompanied by Rhodamine 123 uptake which exceeded 10 nmol/mg of protein or 10 mM in the mitochondrial inner compartment before swelling occurred. Calculated in-to-out concentration ratios approached 4000 : 1. The basic mechanism of energy-dependent uptake appeared to be electrophoretic movement across the inner membrane, since bound-to-free ratios were constant at Rhodamine concentrations which did not cause swelling. Thus, Rhodamine 123 is a redistribution probe, since it redistributes across the membrane under the influence of $\Delta\psi$. However, the mechanism underlying the spectral changes of Rhodamine 123 appears to differ from that for the redistribution responses of a number of other cationic dyes in which dye stacking at the membrane surface is proposed [23–27]. Dye stacking is presumed to occur because of hydrophobic interactions between dye molecules in a polar environment. Stacking is greater at higher dye concentrations and when dye molecules are concentrated locally as at a membrane surface. Spectral changes caused by stacking are a shift in the wavelength maximum of absorbance and a decrease of the extinction coefficient. The changes in the spectral properties of Rhodamine 123 were inconsistent with stacking. No absorbance shifts occurred at high concentrations in water as occurs with other stacking dyes (see Ref. 25), and the energy-linked wavelength shift that did occur was towards the alcohol spectrum – opposite in direction to that expected for stacking. The absence of a decrease in the extinction coefficient following energization also indicated an absence of stacking. A pure binding mechanism is often inferred from linear Scatchard plots indicating of a single class of high-affinity binding sites. However, the present results show that apparently linear Scatchard plots may result if swelling occurs during electrophoretic uptake.

Several lines of evidence indicated that a substantial proportion of internalized dye was bound rather than free. Membrane potentials estimated from measured dye uptake and the Nernst equation exceeded values calibrated by potassium diffusion potentials. Fluorescence polarization increased manifold following energy-linked dye uptake. Finally, dye concentrations in the matrix space greatly exceeded the K_i for inhibition of F_1F_0-ATPase before significant inhibition of ADP-stimulated respiration occurred. DASPMI is another cationic dye which is taken up electrophoretically into mitochondria [28,29]. Like Rhodamine 123 quite high membrane potentials can be calculated from measured DASPMI uptake. This suggests that significant matrix binding of DASPMI also occurs.

Energy-linked spectral red shifts and fluorescence quenching thus appeared to be the consequence of electrophoretic dye uptake followed by

low affinity, high-capacity binding in the matrix compartment. However, red shifts and quenching were not always closely correlated. Values of $\Delta\psi$ inferred from fluorescence quenching generally exceeded values inferred from absorbance red shifts. Large red shifts without quenching were observed with solvents less polar than water and with micellar SDS, whereas quenching without significant red shifts was observed with monomeric SDS, with adenine nucleotides, and with nonenergized mitochondria and purified mitochondrial membrane vesicles. In consideration of all these data, it seems likely that spectral red shifts occurred as a result of a change in polarity of the dye's environment. Quenching appeared to occur as a consequence of pairing of Rhodamine 123 with anions. The amphipathic anion, SDS, was a more potent quencher than the hydrophilic anions, ATP and ADP.

Quantitation of $\Delta\psi$ from the dye signals was problematic. $\Delta\psi$ estimated during State 4 ranged from 181 mV to 212 mV depending on whether absorbance, fluorescence or uptake data were used. The potassium diffusion potential is often relied upon as the most reliable standard with which to calibrate probes of $\Delta\psi$. Calculated potassium diffusion potentials depend on the assumptions that that there are no current carriers of significance through the membrane other than potassium ions, that binding of potassium ions within the matrix does not occur, and that the activity coefficient for potassium ions in the matrix is identical to that in dilute aqueous medium. The matrix environment, however, is quite different from that of the dilute aqueous phase. Protein concentration is greater than 0.5 g per g of water [21]. Allowing for hydration shells of proteins and membranes, there is relatively little free water of solution [30]. As a result, many matrix solutes must either be bound or, equivalently, have diminished activity coefficients.

The chemical activity of Rhodamine 123 within the matrix can be roughly estimated from the inhibition of F_1F_0-ATPase-linked metabolism. In oligomycin titrations from previous studies of the rate control of oxidative phosphorylation [31], 77% inhibition of ATPase was required in order to inhibit ADP-stimulated respiration by 50%. The concentration of Rhodamine 123 inhibiting ADP-stimulated respiration by 50% was 11.8 μM corresponding to an internal Rhodamine 123 concentration of 11 mM (see Fig. 9 and Table II). Since the K_i of Rhodamine 123 for the F_1F_0-ATPase of inverted inner membrane vesicles was 126 μM, 77% inhibition would be achieved at a matrix concentration of 422 μM. The ratio of 422 μM to 11 mM, or 0.038, represents an effective activity coefficient for Rhodamine 123 assuming, of course, that the same inhibitory kinetics apply to ATPase in intact mitochondria as to inverted inner membrane vesicles. Correcting for this activity coefficient, the average Nernst potential from the data of Table II becomes 127 mV. Although this is an approximate calculation, it does suggest the extent to which calculated Nernst potentials may overestimate true mitochondrial potentials. For this reason, Rhodamine 123 is suitable primarily as a qualitative rather than a quantitative indicator of $\Delta\psi$.

Consistent with previous reports [10–12], Rhodamine 123 caused a fairly specific inhibition of ADP-stimulated (State-3) respiration. As a consequence of uptake into the matrix space, much lower concentrations of Rhodamine 123 inhibited ADP-stimulated respiration of intact mitochondria than ATPase of inverted inner membrane vesicles. An analogous observation was made by Modica-Napolitano and co-workers [12] who found that coupled ATP synthesis by isolated mitochondria was much more sensitive to Rhodamine 123 than uncoupled ATPase by the same mitochondria. Other cationic rhodamines, such as rhodamine 6G, and other cationic dyes, such as safranine and DASPMI, are also potent inhibitors of State-3 respiration and oligomycin-sensitive ATPase [10,24,27,28,32]. In the present study, Rhodamine 123 inhibited both oligomycin-sensitive F_1F_0-ATPase of inverted inner membrane vesicles and partially purified, oligomycin-insensitive F_1-ATPase. Mai and Allison [10], in contrast, reported that purified F_1 was insensitive to Rhodamine 123. The reason for this discrepancy is not known.

Above about 15 μM Rhodamine 123, there was some inhibition of uncoupled respiration and stimulation of State-4 respiration. The magnitude of these effects was variable in different experiments and even at 50 μM these effects were small

(data to shown). In inverted inner membrane vesicles, no inhibition of respiration and little loss of respiratory control was observed even at 190 μM Rhodamine 123. Although it has been suggested that Rhodamine 123 may inhibit electron-transfer reactions and cause uncoupling [12], these effects may be secondary to swelling. Mitochondrial swelling was observed beginning at Rhodamine 123 concentrations greater than about 20 nmol/mg of protein (10 μM). Other permeable cation probes did not cause swelling at equivalent or greater concentrations. Thus, Rhodamine 123 may disrupt mechanisms regulating mitochondrial volume control. Additional sites of action are also suggested by studies showing Rhodamine 123 inhibition of precursor protein uptake by mitochondria [33,34].

The present study provides valuable insights concerning Rhodamine 123 labeling of mitochondria in living cells. It is demonstrated directly for the first time that Rhodamine 123 accumulates in response to $\Delta\psi$. However, the nearly 4000-fold concentration gradient which develops is due largely to Rhodamine 123 binding in the matrix compartment. Although the fluorescence of whole suspensions of mitochondria is actually quenched by energization, this is more than offset by the magnitude of Rhodamine 123 uptake such that individual mitochondria as viewed by fluorescence microscopy become intensely fluorescent. Rhodamine 123 staining in situ varies from cell line to cell line. In general, carcinoma and transformed cells lines retain Rhodamine 123 fluorescence longer than nontransformed cell lines [4,6]. It has been suggested that cell lines with greater retention of Rhodamine 123 have a greater mitochondria $\Delta\psi$ [3]. However, the factors controlling Rhodamine 123 binding and quenching are largely unknown, and these may be more important determinants of the magnitude and retention of Rhodamine 123 fluorescence in mitochondria of living cells than $\Delta\psi$.

Other inhibitors of mitochondrial ATPase are potent toxins, and the simplest explanation of the toxicity of Rhodamine 123 in living cells is an inhibition of mitochondrial ATPase, an effect which is magnified manifold by energy-dependent Rhodamine 123 uptake. Other rhodamines which are more cytotoxic are also more potent inhibitors of ATPase [1,2,10,32]. Since metabolism of mitochondria isolated from Rhodamine 123-sensitive and resistant cells is nearly equally inhibited by Rhodamine 123 [13], the differential toxicity of transformed cells in vitro and in vivo may be a consequence of greater retention of Rhodamine 123 and thus longer exposure to it.

Acknowledgements

This work was supported in part by Grants AM37034 and HL35490 from the National Institutes of Health. J.J.L. is an Established Investigator of the American Heart Association.

References

1 Johnson, L.V., Walsh, M.L. and Chen, L.B. (1980) Proc. Natl. Acad. Sci. U.S.A. 77, 990–994
2 Johnson, L.V., Walsh, M.L., Bockus, B.J. and Chen, J.B. (1981) J. Cell Biol. 88, 526–535
3 Johnson, L.V., Summerhayes, I.C. and Chen, L.B. (1982) Cell 28, 7–14
4 Darzynkiewicz, Z., Staiano-Coico, L. and Melamed, M.R. (1981) Proc. Natl. Acad. Sci. USA 78, 2383–2387
5 Darzynkiewicz, Z., Traganos, F., Staiano-Coico, L., Kapuscinski, J. and Melamed, M.R. (1982) Cancer Res. 42, 799–806
6 Summerhayes, I.C., Lampidis, T.J., Bernal, S.D., Nadakavukaren, J.J., Nadakavukaren, K.K., Shepherd, E.L. and Chen, L.B. (1982) Proc. Natl. Acad. Sci. USA 79, 5292–5296
7 Bernal, S.D., Lampidis, T.J., Summerhayes, I.C. and Chen, L.B. (1982) Science 218, 1117–1119
8 Bernal, S.D., Lampidis, T.J., McIsaac, R.M. and Chen, L.B. (1983) Science 222, 169–172
9 Lampidis, T.J., Bernal, S.D., Summerhayes, I.C. and Chen, L.B. (1983) Cancer Res. 43, 716–720
10 Mai, M. and Allison, W.S. (1983) Arch. Biochem. Biophys. 221, 467–476
11 Emaus, R.K., Grunwald, R. and Lemasters, J.J. (1983) J. Cell Biol. 97, 365a
12 Modica-Napolitano, J.S., Weiss, M.J., Chen, L.B. and Aprille, J.R. (1984) Biochem. Biophys. Res. Commun. 118, 717–723
13 Abou-Khalil, S., Abou-Khalil, W.H., Planas, L., Tapiero, H. and Lampidis, T.J. (1985) Biochem. Biophys. Res. Commun. 127, 1039–1044
14 Lemasters, J.J., Grunwald, R. and Emaus, R.K. (1984) J. Biol. Chem. 259, 3058–3063
15 Lemasters, J.J. (1980) FEBS Lett. 110, 96–100
16 Linnett, P.E., Mitchell, A.D., Partis, M.D. and Beechey, R.B. (1979) Methods Enzymol. 55, 327–334
17 Gornall, A.G., Bardawill, C.J. and David, M.M. (1949) J. Biol. Chem. 177, 751–766
18 Lowry, O.H., Rosebrough, N.J., Farr, A.L. and Randall, R.J. (1951) J. Biol. Chem. 193, 265–275

19 Lemasters, J.J. and Billica, W.H. (1981) J. Biol. Chem. 256, 12949–12957
20 Rossi, E. and Azzone, G.F. (1969) Eur. J. Biochem. 7, 418–426
21 Hackenbrock, C.R. (1968) Proc. Natl. Acad. Sci. USA 61, 589–605
22 Corrin, M.L. and Harkins, W.D. (1947) J. Am. Chem. Sco. 69, 679–683
23 Yaginuma, N., Hirose, S. and Inada, Y. (1973) J. Biochem. 74, 811–815
24 Gear, A.R.L. (1974) J. Biol. Chem. 249, 3628–3637
25 Colonna, R., Massari, S. and Azzone, G.F. (1973) Eur. J. Biochem. 34, 577–585
26 Akerman, K.E.O. and Wikström, M.K.F. (1976) FEBS Lett. 68, 191–197
27 Zanott, A. and Azzone, G.F. (1980) Arch. Biochem. Biophys. 201, 255–265
28 Bereiter-Hahn, J. (1976) Biochim. Biophys. Acta 423, 1–14
29 Mewes, H.-W. and Rafael, J. (1981) FEBS Lett. 131, 7–10
30 Srere, P.A. (1980) Trends Biochem. Sci. 5, 120–121
31 Grunwald, R. and Lemasters, J.J. (1982) EBEC Short Rep. 2, 269–270
32 Higuti, T., Niimi, S., Saito, R., Nakasima, S., Ohe, T., Tani, I. and Yoshimura, T. (1980) Biochim. Biophys. Acta 593, 463–467
33 Morita, T., Mori, M., Ikeda, F. and Tatibana, M. (1982) J. Biol. Chem. 257, 10547–10550
34 Oda, T., Ichiyama, A., Miura, S. and Mori, M. (1984) J. Biochem. 95, 815–824